

## Observation of radiation damage in CdTe Schottky sensors created by 20 keV photons

M. Meyer,<sup>a</sup> M. Andrä,<sup>a</sup> R. Barten,<sup>a</sup> A. Bergamaschi,<sup>a</sup> M. Brückner,<sup>a</sup> P. Busca,<sup>b</sup>  
M. Carulla Areste,<sup>a</sup> S. Chiriotti,<sup>a</sup> R. Dinapoli,<sup>a</sup> P. Fajardo,<sup>b</sup> E. Fröjd, <sup>a</sup> D. Greiffenberg,<sup>a,\*</sup>  
J. Heymes,<sup>a</sup> V. Hinger,<sup>a</sup> P. Kozlowski,<sup>a</sup> C. Lopez-Cuenca,<sup>a</sup> D. Mezza,<sup>a</sup> A. Mozzanica,<sup>a</sup>  
S. Redford,<sup>a</sup> M. Ruat,<sup>b</sup> C. Ruder,<sup>a</sup> B. Schmitt,<sup>a</sup> D. Thattil,<sup>a</sup> G. Tinti,<sup>a</sup> S. Vetter<sup>a</sup> and J. Zhang<sup>a</sup>

<sup>a</sup>Paul-Scherrer-Institute (PSI),  
Villigen PSI CH-5232, Switzerland

<sup>b</sup>European Synchrotron Radiation Facility (ESRF),  
Avenue des Martyrs, Grenoble F-38043, France

E-mail: [dominic.greiffenberg@psi.ch](mailto:dominic.greiffenberg@psi.ch)

**ABSTRACT:** The polarization characteristics of ohmic and (Al-)Schottky type CdTe sensors supplied by Acrorad have been characterized with the low noise, charge integrating readout chip JUNGFR AU, revealing defined areas in the Schottky type sensors, which were irradiated with 20 keV photons in previous experiments more than one year ago. These areas, which have absorbed doses of up to 1079 kGy, show a more robust charge collection compared to unirradiated areas. In contrast to this, no alteration of the polarization characteristics could be found in ohmic type CdTe sensors after irradiation. The polarization behavior of the sensors has been characterized in-situ over time and at different temperatures by using an homogeneous, low flux molybdenum fluorescence illumination. An increase of the leakage current in the irradiated areas was found and quantified as a function of absorbed dose as well as its influence on the stability on the number of photon counts. In addition to the influence of X-ray irradiation, the effect of thermal annealing on the polarization characteristics of Schottky type CdTe sensors has been studied. Possible routes for the usage of Schottky type CdTe sensors in synchrotron applications are outlined in this publication.

**KEYWORDS:** Hybrid detectors; Instrumentation for FEL; Instrumentation for synchrotron radiation accelerators; X-ray detectors and telescopes

\*Corresponding author.



---

## Contents

<b>1</b>	<b>Introduction</b>	<b>1</b>
<b>2</b>	<b>Material and methods</b>	<b>3</b>
2.1	CdTe sensors under investigation and their irradiation history	3
2.2	Operating conditions	3
2.3	Data analysis	4
<b>3</b>	<b>Description of the effect caused by bias-induced polarization</b>	<b>5</b>
<b>4</b>	<b>Influence of irradiation and thermal annealing on polarization characteristics</b>	<b>11</b>
4.1	Effect of irradiation with monochromatic 20 keV photons	11
4.2	Effect of irradiation at the X-ray tube with an acceleration voltage of 25 kV	14
4.3	Comparison with ohmic type CdTe sensors	15
4.4	Effect of thermal annealing at +80°C	17
4.5	Comparison between different batches of electron collecting Schottky CdTe sensors	18
<b>5</b>	<b>Conclusion</b>	<b>19</b>

---

## 1 Introduction

High-Z sensors are of great interest for the detection of X-rays with a photon energy above 20 keV. In contrast to silicon, which is the most common sensor material for detectors at synchrotron sources and free electron lasers, the absorption efficiency of high-Z sensors is more adequate in a broader range of X-ray energies. Suitable efficiencies can be achieved at photon energies even above 100 keV depending on the material composition and the thickness [1]. Possible applications are reported for astronomy, medicine, homeland security and material science [2]–[5].

These materials, however, suffer from shortcomings like dislocation lines, charge-trapping and high energy fluorescence photons. They do not provide the same performance as silicon-based sensors especially in terms of charge transport properties and crystal homogeneity [6]–[8]. Among the available high-Z semiconductor sensor materials, the crystal quality of CdTe improved in recent decades [9]–[11]. Sensors made from CdTe provide a high resistivity at room temperature as well as a large linear attenuation coefficient.

Two of the most common contact configurations used in combination with CdTe sensors are (quasi-) ohmic type (Pt/CdTe/Pt) and hole-blocking Schottky type (Al/CdTe/Pt) contacts (figure 1) [12]. Ohmic type CdTe sensors show a stable charge collection behavior in time, but have a high dark current, while the latter, which have a very low leakage current, suffer from polarization issues with increasing biasing time [13, 14].

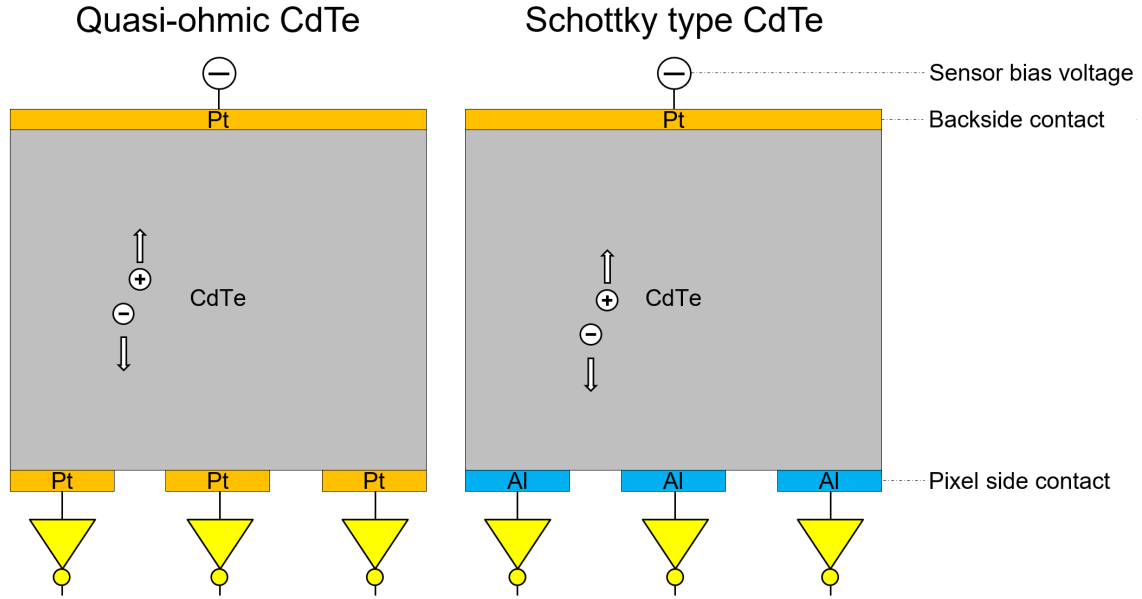


**Figure 1.** (Left) Quasi-ohmic type CdTe sensor with platinum contacts on both the backside and the pixel side. (Right) Electron collecting Schottky type CdTe sensor with a backside contact made of platinum and with aluminum pixel side contacts forming a hole blocking Schottky contact.

CdTe sensors with ohmic contacts act as photoresistors, thus charge carriers of either polarity can be injected, which is the reason why ohmic type CdTe sensors show stable charge collection properties and typically do not suffer from polarization caused by solely biasing the sensor (bias-induced polarization). However, one of the major drawbacks of ohmic CdTe sensors is the relatively high dark current through the sensor, which is defined by the resistivity of the CdTe [13].

A rectifying behavior is achieved by replacing one of the ohmic contacts with a Schottky contact, thus reducing the current through the sensor. When collecting electrons, aluminum can be used as contact material on the pixel side, preventing the injection of holes from the pixel side. A drawback of this contact configuration is that Schottky type CdTe sensors with aluminum contact on the pixel side suffer from bias-induced polarization. This is commonly attributed to the ionization of deep acceptors close to the readout contacts, which is present after biasing the detector for several hours [14]–[16]. Negative space charges are left behind in the bulk because of hole detrapping (and a lack of re-injecting holes through the hole-blocking pixel side contact) causing changes in the electric field distribution [17]. The resulting performance degradation is well-known since the 1970s [18].

A measurement campaign was performed at the MS beamline of the Swiss Light Source (SLS) [19], where 16 areas of roughly  $1.2 \times 2 \text{ mm}^2$  have been irradiated with monochromatic 20 keV photons to 16 different doses, ranging between 0.01 kGy and 1079 kGy. Remarkably, one year after these experiments took place, changes of the polarization behavior of the Schottky CdTe sensors were observed. Depending on the absorbed dose, the effect of the bias-induced polarization was reduced in the areas which previously have been irradiated and the charge collection was more robust. On the contrary, measurements with ohmic type CdTe of the same thickness did not show any changes of the charge collection behavior of the irradiated areas with respect to the unirradiated parts of the sensors.

The charge-integrating JUNGFRÄU readout chip providing  $256 \times 256$  readout channels with a pixel pitch of  $75 \mu\text{m}$  was used for the sensor characterization. Details on the JUNGFRÄU readout application-specific integrated circuit (ASIC), developed at PSI, have been published and described in detail elsewhere [20]. The choice of using a charge integrating readout chip is motivated by its capability to precisely measure the charge induced in the contacts during a pre-defined integration time thus enabling a detailed analysis.

The paper is structured as follows: in the first part of the paper the polarization behavior of unirradiated areas of the Schottky CdTe sensor is characterized and compared to ohmic CdTe sensors in order to define a standard polarization behavior. In the following, the change of the polarization behavior is evaluated for the irradiated areas as a function of temperature and dose. In order to exclude radiation effects to the readout chip and/or the Schottky contact on the pixel side due to the higher penetration depth of higher harmonic photons at the beamline, a specific area was irradiated using an X-ray tube with an acceleration voltage of 25 kV, so that a shallow absorption profile of the photons is ensured. In an attempt to thermally anneal the Schottky CdTe sensor at  $+80^\circ\text{C}$ , changes of the polarization behavior (of previously unirradiated areas) were found and subsequently characterized.

## 2 Material and methods

### 2.1 CdTe sensors under investigation and their irradiation history

In this study CdTe sensors supplied by Acrorad Co., Ltd., Japan were used [21]. The thickness of all CdTe sensors presented in this study is  $750 \mu\text{m}$ . Flip-chip bonding was performed by Advacam [22]. High voltage with negative polarity was supplied by an external voltage source to the backside in order to collect electrons at the readout electrodes (figure 1).

The electron collecting Schottky type sensors consist of a quasi-ohmic Pt-contact on the backside and a structured Al contact on the pixel side ( $256 \times 256$  pixels of  $75 \times 75 \mu\text{m}^2$ ). The ohmic type sensors are layered between two thin quasi-ohmic contacts made of Pt.

In this study, Schottky type sensors delivered in 2019 were investigated in detail and compared to ohmic type sensors (also from 2019), as well as Schottky type sensors obtained earlier in 2017. All presented sensors had already been used in previous measurement campaigns at the MS beamline of the SLS. The results of these experiments will be published later and are not part of this publication. 20 keV monochromatic photons were used to irradiate well-defined rectangular areas shaped by slits to sizes of around  $1.2 \times 2 \text{ mm}^2$ . The photon fluxes were varied by means of silicon filters and covered fluxes from  $1.1 \times 10^7 \text{ ph/mm}^2/\text{s}$  up to  $7.2 \times 10^{10} \text{ ph/mm}^2/\text{s}$  with integrated doses ranging from 0.01 to 1079 kGy. An overview of the irradiation geometry with the estimated fluxes and deposited doses in the respective areas is given in figure 2. Category A areas were irradiated for a total of 213 seconds, areas assigned to category B were irradiated for 2400 seconds.

Bulk damage [23], as well as damage to the readout chip and/or an alteration of the pixel side contacts (being the rectifying contacts) can be excluded due to the low penetration depth of the 20 keV photons of around  $80 \mu\text{m}$  (absorption length) in CdTe.

### 2.2 Operating conditions

All test assemblies, consisting of single JUNGFRÄU1.0 ASICs bump bonded to correspondingly sized sensors, were operated with a 500k JUNGFRÄU single module system with a gentle nitrogen

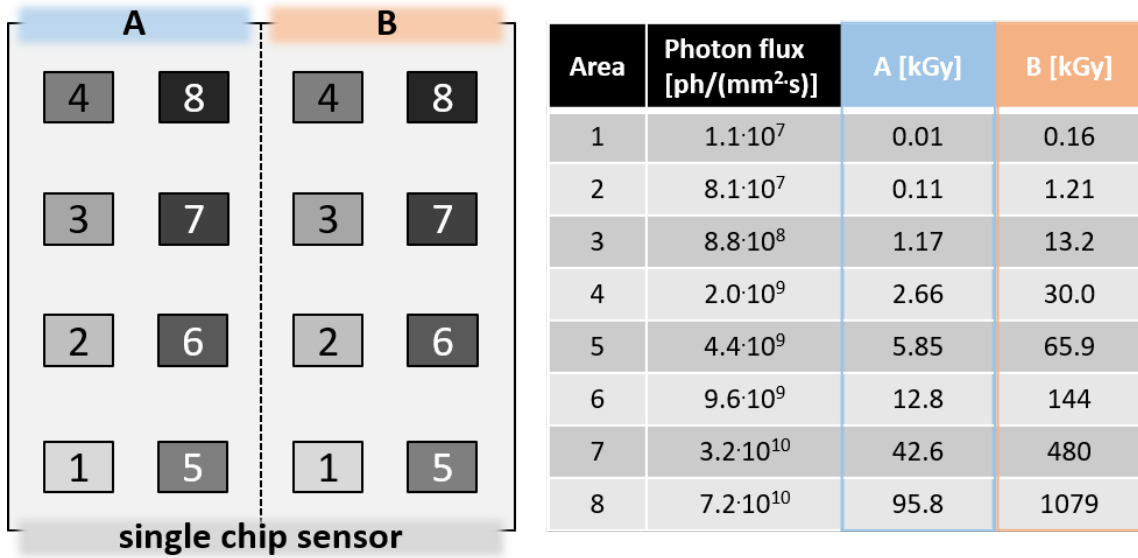


**Figure 2.** Geometrical arrangement of single  $2 \times 2 \text{ cm}^2$  sensors of previous measurements performed at the MS beamline. The table (right) gives an overview on the estimated fluxes and doses deposited in each area.

flow to avoid condensation on the front-end module (sensor + ASIC) also at temperatures down to  $0^\circ\text{C}$ . The operating temperature was controlled by a water-cooling system with set-values between  $0^\circ\text{C}$  and  $30^\circ\text{C}$  ( $\pm 0.1^\circ\text{K}$ ). The bias voltage was supplied by an external high voltage source (Keithley 6487) to a typical value of  $-500 \text{ V}$ , resulting in an average strength of the electric field of  $660 \text{ kV/cm}$ . Each sensor was not biased for a period of at least 15 minutes right before the start of each experiment to ensure comparability between the experiments. If not specified differently, data taking was performed at a frame rate of  $500 \text{ Hz}$ . Due to the higher dark current of the ohmic type sensors and in order to ensure a sufficient dynamic range of the front-end electronics, an integration time of  $5 \mu\text{s}$  was chosen for the ohmic type sensors, shorter than the  $15 \mu\text{s}$  used with Schottky type sensors. Most of the measurements presented in this publication rely on data obtained by a uniform illumination of the CdTe sensors with X-ray fluorescence from molybdenum ( $17.4 \text{ keV}$ ). The photon flux was chosen low enough to ensure a low occupancy of photon hits on the pixel array.

### 2.3 Data analysis

The data output of the charge-integrating JUNGFRÄU ASIC was corrected on a pixel-by-pixel basis for the so-called pedestal, which is the value of the pixel output in a dark frame. The pedestal is mainly determined by the working point of the ASIC as well as the sensor leakage current collected during the integration time. The observed dynamic fluctuations in the pedestal are addressed by pedestal tracking (basic principle is described in [24]) and a common mode correction along the x- and y-axis. Pedestal tracking is useful for pedestal drift corrections during the experiment in a low photon flux environment, when most pixels per frame are not hit by incoming photons. The mean value of the first 2000 frames served as a starting point for the pedestal tracking in each experiment. The drift correction by pedestal tracking is necessary as the pedestal drift due to polarization effects at higher temperatures is not negligible. While applying pedestal tracking and

common mode corrections improves the energy resolution and noise of the system, the corrections are small ( $< \pm 1$  keV), so no systematic errors are introduced.

Albeit JUNGFRU is a charge-integrating readout chip, an algorithm with an off-line threshold was added to the data treatment to mimic a single photon counting detector (SPCD). This enables the comparison of our results to those obtained with SPDs [7, 11, 12].

A cluster finding algorithm was used to detect photon hits and to assign the photon hits to the pixel with the highest signal within  $3 \times 3$  pixel clusters (details in [24]). A photon counting detector (with charge sharing suppression) was mimicked in software to track the number of photon hits by defining a threshold for the  $3 \times 3$  cluster sum of 450 ADU (about 12.8 keV) in the analysis. This threshold, corresponding to roughly 2/3 of the incoming photon energy, was held constant throughout this study to simulate practical measurements where a stable signal is present and thus a fixed threshold is applied. The photon hit finding was performed on a frame-by-frame basis and is valid only in a low-flux environment. 2-dimensional photon hit maps were generated by summing up all photon hits identified on a pixel-by-pixel basis in a constant number of consecutive frames, typically corresponding to the number of frames obtained in 1 minute (30000 frames). Additionally, the contribution of all pixels within the assigned  $3 \times 3$  cluster were excluded from the common mode correction as well as from the pedestal tracking.

### 3 Description of the effect caused by bias-induced polarization

In this section we compare the polarization behavior found in the CdTe sensors with different contact configurations (Schottky: Al/CdTe/Pt, Quasi-ohmic: Pt/CdTe/Pt) supplied by AcroRad.

An X-ray tube was used to illuminate a molybdenum foil to create a low flux environment (i.e.,  $10^4$ – $10^5$  ph/mm<sup>2</sup>/s) of 17.4 keV fluorescence photons in order to generate continuous and uniform photon hit maps of the biased sensors.

In the following, when referring to the normalized number of photon hits, the number of photons counted by each pixel was normalized to the average number of photon hits within the 1<sup>st</sup> minute over the entire sensor (as the sensor was uniformly illuminated). Within the 1<sup>st</sup> minute the distribution of the normalized number of photon hits shows the expected Gaussian profile, arising from statistical Poisson fluctuations as well as pixel to pixel variations. As the impinging irradiation from the X-ray tube can be approximated to be constant over time, deviations monitored on a pixel-by-pixel basis are therefore likely related to changes in the sensor response itself. This process was repeated for Schottky and quasi-ohmic type sensors at different temperatures by creating normalized photon hit maps for each minute after biasing the sensor. From the normalized photon hit maps, the distribution of the normalized photon hits was plotted, and each pixel was assigned to a category [table 1] depending on its normalized number of counts with respect to the initial average value over the entire sensor.

Figure 3 (left column) shows the normalized photon hit maps after 5 h in low flux conditions for a Schottky type sensor at three different temperatures. The central column of figure 3 shows the distribution of the normalized number of hits over the sensor at different times after the start of the experiment (0/60/120/180/240/300 minutes), extracted from the corresponding normalized photon hit maps (left column). This representation allows to visualize the trends over time which are present in the sensor during (low flux) irradiation, so that the complex multidimensional data

**Table 1.** Assignment of pixels to a category according to their counting behavior, indicated as a colored area in the central column and differently colored lines in the right column of figure 3 using the color code from this table.

Assignment	Normalized number of photon hits	Color code
Very low	<50%	Blue
Low	50% . . . 80%	Green
Average	80% . . . 120%	Black
High	120% . . . 150%	Orange
Very high	>150%	Red

can be interpreted. Depending on the temperature of the sensor, the normalized number of photons hits decreases, globally over the pixel array, over time. This is a known effect which is commonly attributed to bias induced polarization in CdTe Schottky sensors [25]. As can be seen in the normalized photon hit maps, this global decrease has strong local variability. The plots shown in figure 3 (right column) give an overview of the number of pixels assigned to the respective category for each minute.

The observed polarization effect in Schottky type CdTe sensors strongly depends on the temperature as presented in figure 3. The sensor shows a uniform distribution of photon hits in the first minute at all three temperatures, when being irradiated with 17.4 keV photons originating from molybdenum fluorescence. At 0°C, after five hours of operation, hardly any signs of polarization are visible in the photon hit map, a conclusion which is reflected in an unvarying statistical output over time. Vice versa, the investigated sensor shows an onset of polarization (indicated by a reduction of normally counting pixels in the range between 80% and 120%) after 35 min at +30°C (black line, figure 3 right). Correspondingly, the number of pixels with very low photon counts increases and after around 70 minutes 99% of the pixels count less than 50% of the initial average value over the whole sensor (blue line). The situation observed at +15°C is in between these extremes, with the sensor showing clear signs of polarization taking effect after 200 minutes of operation. These observations indicate the temperature related dependency of the polarization process. Moreover, it is noteworthy, that repetitions of the measurements lead to reproducible spatial patterns of the normalized photon hit maps which points to an unknown underlying local effect influencing polarization.

Figure 4 shows the same figures of merit for an ohmic type sensor. In contrast to the behavior of a Schottky type CdTe sensor, no change in the overall photon hit distribution can be found (beyond statistical variations) even after being biased for 5 h at +30°C. Our dataset is in good agreement with literature, stating no signs of bias-induced polarization in CdTe sensors with ohmic contacts [26]. Please note that the artifacts at the beginning of the data acquisition arise from the relatively slow transients of the dark current until the sensor equilibrium is reached and the data processing like pedestal tracking works reliably (i.e., 10 min, to fully recover all photon hits). After the equilibrium state of the dark current is reached after around 60 minutes, no further changes are observed in the overall sensor behavior. Therefore, for the ohmic type sensors the average photon hit map response at 60 min serves as reference value for 100%.

The observations in the present study are mainly assigned to bias-induced polarization (in contrast to photon induced polarization). In order to validate the assumption that a low photon flux

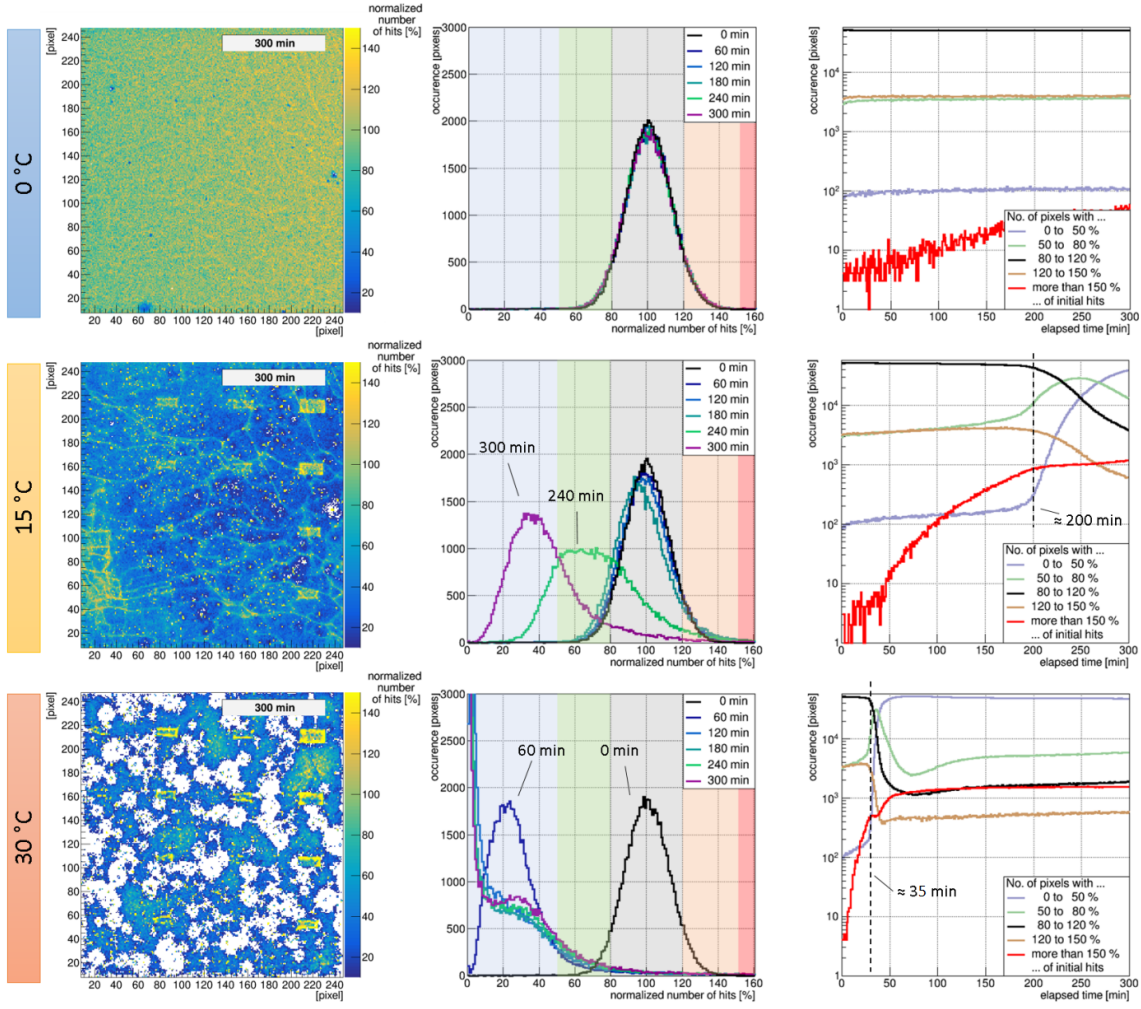


**Figure 3.** (Left) Normalized photon hit maps of a Schottky type CdTe sensor at different temperatures after 5 h operated at  $-500$  V in a low flux environment. The z-axis shows the relative number of photon hits, normalized to the average photon hit rate within the first minute of illumination, i.e. before polarization. White areas in the photon hit map represent values below 10% of the initial photon hits. (Center) The corresponding distribution of the normalized number of hits in percent (100% corresponds to the initial average number of hits per pixel over the entire sensor) at certain time stamps. (Right) Evaluation of the pixel hit distribution according to the normalized number of counts versus experiment time: 0–50% of initial hits: very low — blue; 50–80%: low — green; 80–120%: nominal — black; 120–150%: high — orange; above 150%: very high — red.

does not alter the polarization characteristics, a reference measurement was set up by performing two measurements using the same biasing conditions: in the first experiment the sensors were continuously irradiated by fluorescence photons from the very beginning for a duration of five hours, whereas for the second measurement the fluorescence was only turned on for 1 minute after five hours of biasing the sensor. In order to show the behavior of single pixels in terms of the evolution of their pedestal and pulse height, a small representative area (region of interest or ROI,  $11 \times 11$  pixels) was chosen for the analysis (figure 5(a)).

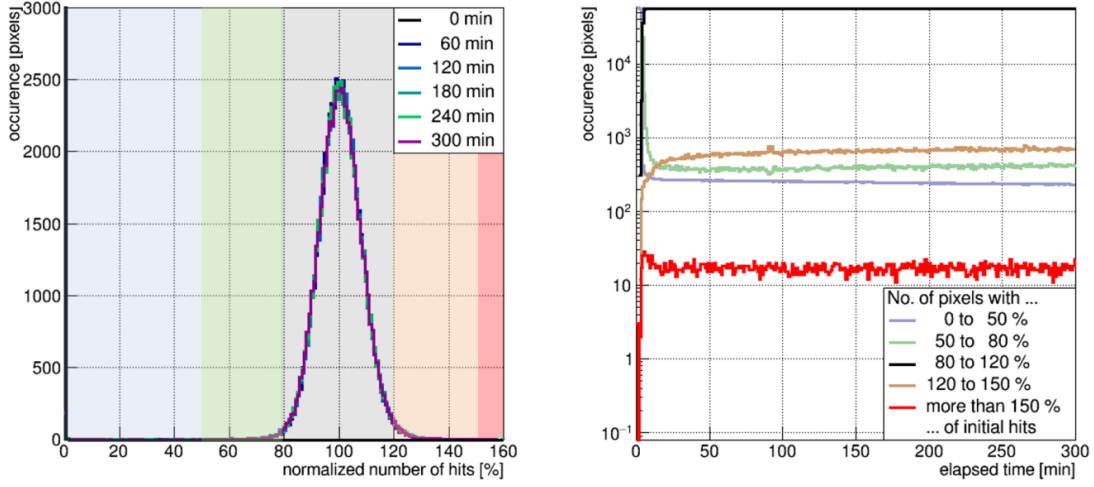


**Figure 4.** (Left) Pixel hit distribution of an ohmic type CdTe sensor operated at  $-500$  V in a low flux environment at  $+30^{\circ}\text{C}$ . (Right) Evaluation of the pixel hit distribution according to defined categories versus experiment time: 0–50% of initial hits: very low — blue; 50–80%: low — green; 80–120%: nominal — black; 120–150%: high — orange; above 150%: very high — red.

At the beginning of the first experiment an overall uniform response of all pixels is observed as shown in figure 5(a) (3D-histograms with all 121 pixels unfolded on the x-axis with pulse height spectra in y direction and occurrence in z-direction). Besides a prominent pedestal peak, all pixels show charge sharing events up to the full photon charge, corresponding to an ADC value of about 610 ADU. The inset in figure 5(a) shows a pulse height histogram (i.e., y-projection over all pixels for better statistics). For these measurements, the pedestal correction was applied using the respective pedestal values of the 1<sup>st</sup> minute of data taking. Pedestal tracking was not used to prevent the tracking mechanism to suppress the pedestal drift.

Comparing the change of the pedestal corrected pulse height spectra of single pixels over time clearly reveals the impact of polarization on a Schottky type sensor (continuous illumination, 0 min: figure 5(a), 300 min: figure 5(b)): the uniform response of all pixels within the region of interest at the beginning turns over into many cold pixels (no photo peak or charge sharing tail visible), barely collecting any charge. On the other hand, a situation best described as a sink is formed (figure 5(d)), where the pixels in the center of the region of interest continuously collect far more charge carriers than at the beginning, with one pixel in its center even saturating. A potential explanation could be that the photo generated charge carriers of the cold pixels are attracted and ultimately collected by the hot pixels.

Figure 5(c) shows the resulting single pixel spectra of the same region of interest measured during 1 minute of X-ray illumination after being biased for five hours without X-rays. When comparing the pulse height spectra with the spectra recorded in a continuous low flux condition (figure 5(b)), no obvious differences are noticeable: this strongly indicates that the observed phenomenon is to a large extent related to bias-induced polarization and the presence of the low photon flux is negligible.

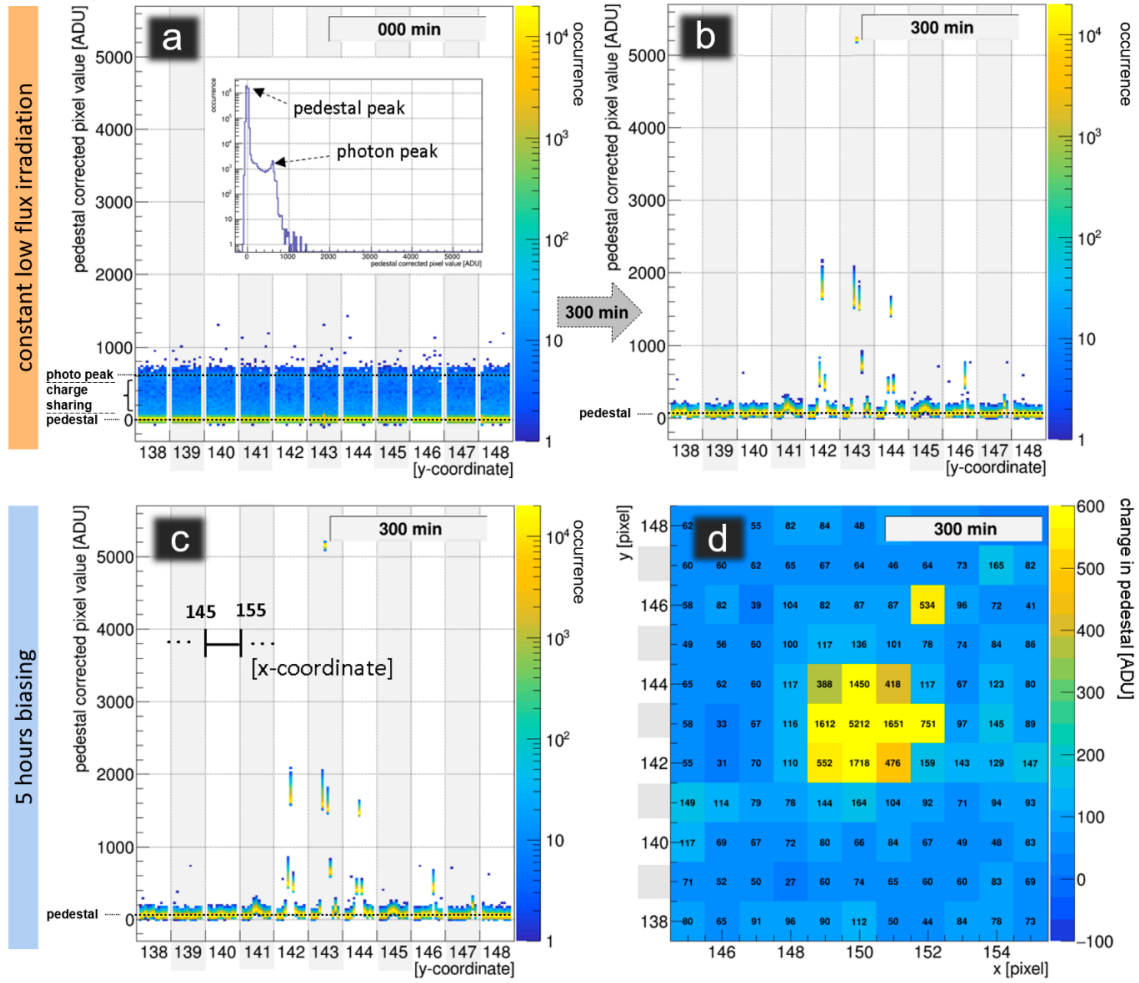


**Figure 5.** (a), (b) Pedestal corrected output (without pedestal tracking) of a Schottky type CdTe sensor (ROI) constantly operated for 5 h at  $-500$  V and at  $+30^\circ\text{C}$  in low flux conditions, the corresponding pulse height spectra for all pixels (inset) and for each individual pixel at the beginning (a, 0 min) and end (b, 300 min). (c) For comparison, the pulse height spectra of the same sensor is shown right after turning on the X-rays after 5 hours of biasing. (d) 2D pedestal corrected output (pedestal value after 1 minute of being biased) of a Schottky type CdTe sensor (ROI) operated for 5 h at  $-500$  V and at  $+30^\circ\text{C}$  in low flux conditions.

Moreover, it is worth to note that all pixels collectively show a higher leakage current after five hours as shown in figure 5(b) and 5(c), indicated by the slight increase of their pedestals.

The increased pedestal values as a measure for a higher leakage current can also be confirmed by the current reading of the high voltage sensor power supply (Keithley 6487) monitored over time. As figure 6 shows, the evolution of the leakage current strongly depends on the temperature when only bias is applied to the sensor.

In search of the origin of the lines structure visible in the photon hit maps of polarized sensors (figure 3, left), the observed polarization pattern was compared to a network of lines present in the Schottky CdTe sensors at the beginning of the polarization process, assigned by other authors to a network of sub-grain boundaries [13]. The sub-grain boundary network was extracted from a photon hit map plot shortly after the onset of polarization (example shown in figure 7(a)) sensing

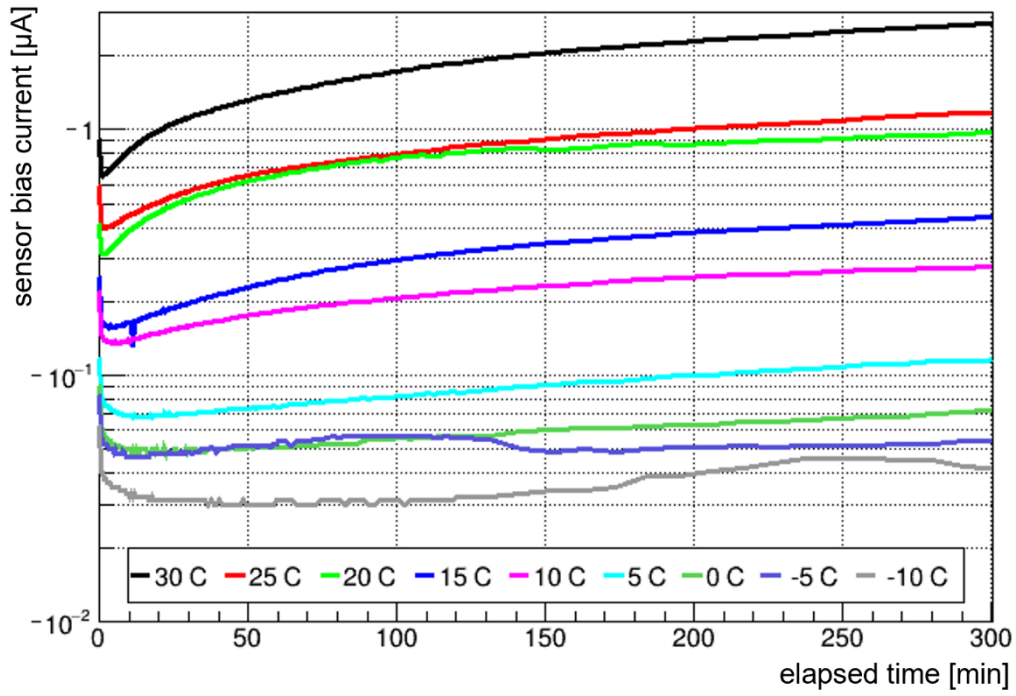


**Figure 6.** Increase of leakage current measured at  $-500$  V for Schottky type CdTe sensor at different temperatures.

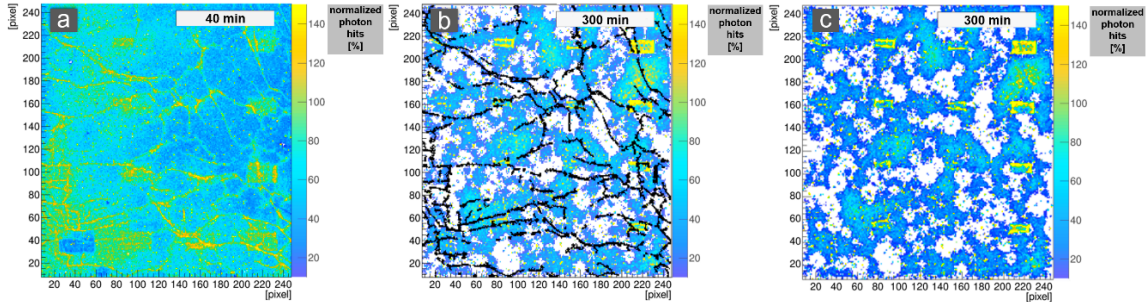


**Figure 7.** Response map of a Schottky type CdTe sensor at  $+30^{\circ}\text{C}$  operated at  $-500$  V in low flux conditions; (a) after 40 min with a clearly visible network of (green) lines, (b) after 300 min overplotted with the (assumed) network lines extracted from the left plot and (c) after 300 min without the overplotted extracted network lines.

strong variations of photon counts (i.e., the normalized number of photon hits of a pixel exceeding the average of its  $9 \times 9$  environment). In a second step, hot pixels were excluded, and the rims of the areas heavily irradiated in the previous MS-experiments were excluded to be part of the line network. However, no correlation between the map of the dislocation line network and the structures visible in a polarized sensor can be seen, as shown in figure 7(b). Hot pixels (not shown) and no/low-count areas (white) are distributed and not predominantly linked to the network lines (black).

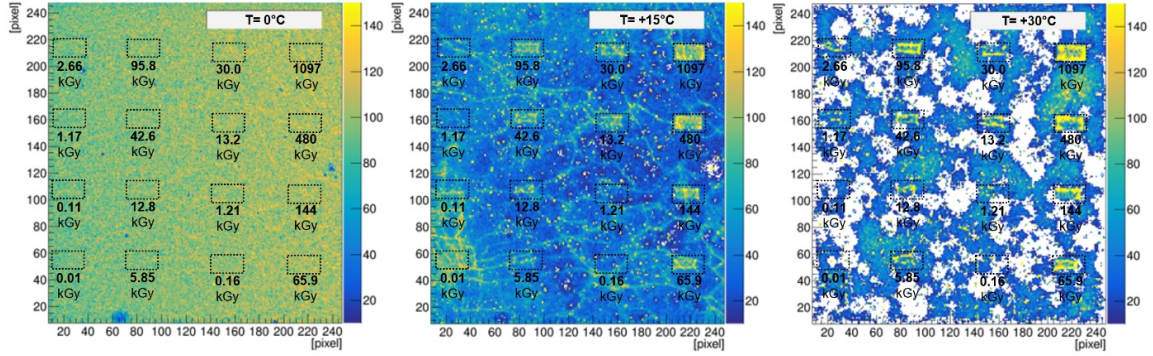


**Figure 8.** Photon hit map after 300 minutes of low flux irradiation and continuously applied high voltage. The 16 areas irradiated in previous measurements are indicated with the dashed boxes and the corresponding dose. (Left) Stable counting behavior of the whole sensor after 300 minutes with a sensor temperature of 0°C. (Center/Right) Depending on the dose absorbed in the previous measurements, the photon counts in the irradiated areas are high after 300 minutes, in contrast to the unirradiated areas of the sensor (center:  $T=+15^{\circ}\text{C}$ /right:  $T=+30^{\circ}\text{C}$ ).

#### 4 Influence of irradiation and thermal annealing on polarization characteristics

In this section we report two factors that we found to influence the polarization characteristics significantly: photon irradiation and thermal annealing of the sensor.

##### 4.1 Effect of irradiation with monochromatic 20 keV photons

Figure 8 shows the (previously shown) maps of the normalized photon counts after 300 minutes of continuous low flux irradiation and continuously applied high voltage for three different temperatures (like figure 3 (left)), marking the areas which were irradiated one year earlier. In the case where polarization effects occur at  $+15^{\circ}\text{C}$  and  $+30^{\circ}\text{C}$ , areas which were (partly intensively) irradiated with 20 keV photons one year earlier, can easily be identified as they reach significantly higher photon counts compared to the unirradiated areas (see dashed boxes which mark the irradiated areas).

Figure 9 shows the counting behavior as well as the pulse height spectra for the area which has received the highest dose of 1079 kGy, indicating its altered polarization behavior compared to the (previously described) unirradiated areas. Pixels outside of the irradiated area (figure 9, left) serve as reference: after the onset of the polarization process (after around 35 minutes), the photo peak signal smears out and the number of detected photons decreases. In contrast, the irradiated area shows a more stable counting behavior as well as being able to maintain a stable pulse height. Note that an increase in the number of photon hits followed by a strong decrease is most likely due to the handling of saturated pixels by the photon finder algorithm.

The area irradiated at the beamline was divided in two regions: a 6 pixel wide rim region and the inner region. In the rim area (figure 9, center), many pixels register significantly more counts after the onset of the polarization and collect more charge compared to the non-irradiated pixels. The pulse height plots as a function of time show a clear, relatively stable photopeak at the nominal value of 610 ADU with a relatively uniform distribution of (partially) collected charge, reaching pulse heights up to 1200 ADU corresponding to the charge of two photons ( $= 2 \times 610 \text{ ADU}$ ). Pixels located in the interior of the irradiated area appear to be more stable over time with a slow decrease

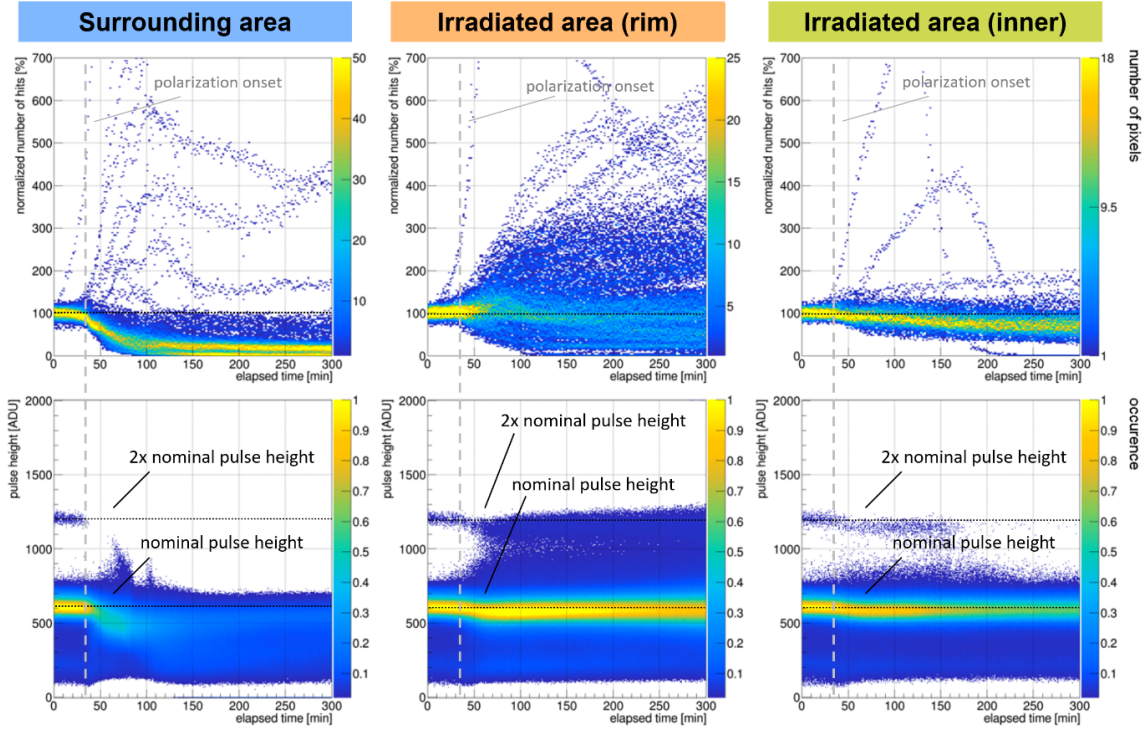
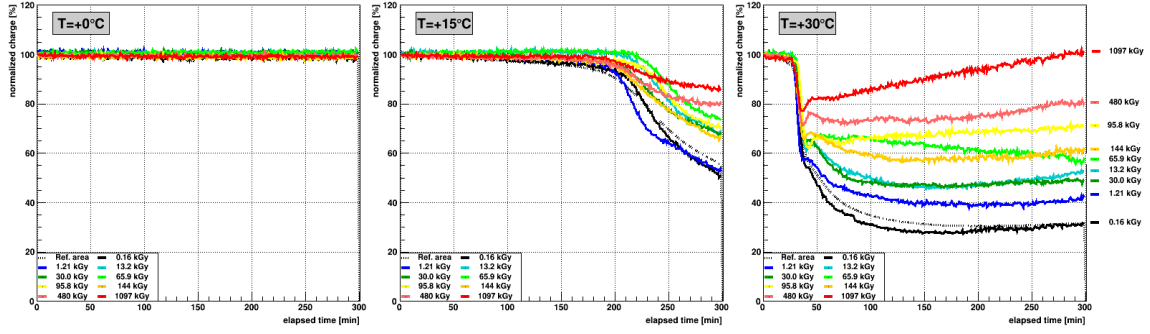


**Figure 9.** Normalized number of photon hits per pixel (top) and the corresponding pulse height histogram (bottom) for the inner part of the irradiated area (right), the rim (center) and its direct surrounding (left) for a Schottky type CdTe sensor at a temperature of  $+30^{\circ}\text{C}$ . Pixels at the rim area count significantly more photon hits after polarization. The area was irradiated with a dose of 1079 kGy. Pedestal tracking was used for the data analysis.

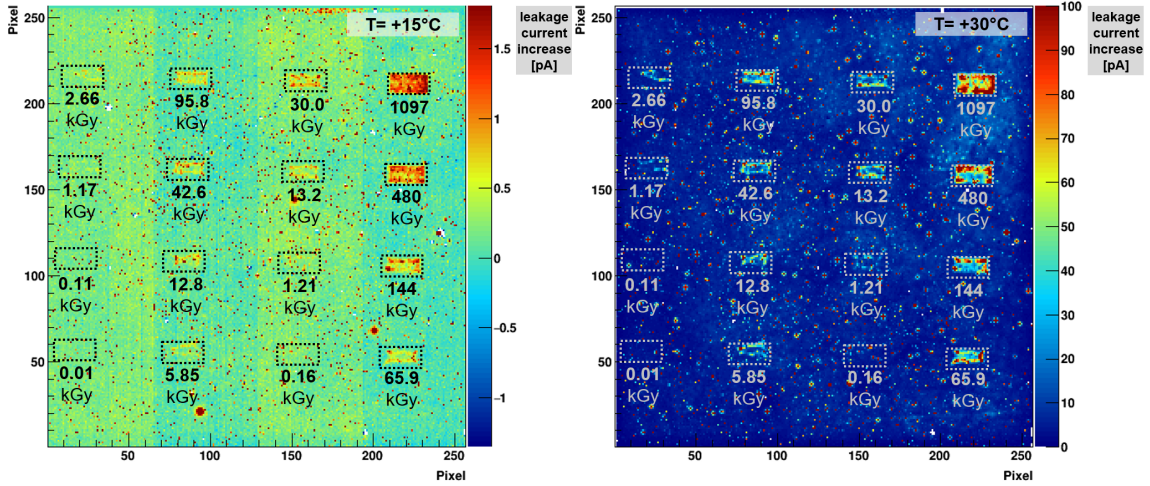
in the number of hits as well as in the pulse height (figure 9, right). A possible explanation of this behavior is that pixels in the border attract charge from polarized areas of the sensor.

Figure 10 shows the collected charge of different irradiated areas normalized to the average charge of the respective area collected within the first minute of operation as a function of the measurement time. The different areas (as depicted in figure 8) were irradiated to doses between 0.16 kGy and 1079 kGy at the beamline one year prior to the measurements presented in this paper. Again, the sensor has been probed with fluorescence photons from molybdenum with a low photon flux for a total of 300 minutes at three different temperatures ( $0^{\circ}\text{C}/+15^{\circ}\text{C}/+30^{\circ}\text{C}$ ). In agreement with the previous measurements, a decrease of collected overall charge sets in after around 200 minutes and after around 35 minutes for  $T = +15^{\circ}\text{C}$  and  $T = +30^{\circ}\text{C}$ , respectively. At  $T = +30^{\circ}\text{C}$ , the collected charge starts to decrease simultaneously for all regions after 35 minutes, however the regions with higher doses recover from this initial drop, and the regions which have collected the highest doses of 480 kGy (light red) and 1097 kGy (red) reach, after 300 minutes, 80% and 100%, respectively, of the nominal charge.

Besides the higher charge collection of the irradiated areas in the polarized state, the development of the leakage current during polarization differs significantly from non-irradiated reference areas. As already stated before, an overall increase of the pedestal (corresponding to a higher leakage current) was found as a subsidiary effect of polarization (figure 11).



**Figure 10.** Normalized charge as function of irradiation time for regions irradiated to different doses. The black dashed line corresponds to a reference area without prior irradiation at the beamline. The irradiation doses vary between 0.16 kGy up to 1079 kGy. (Left) Sensor temperature of 0°C. (Center) Sensor temperature of +15°C. In accordance with the previous observations (the counts drops after 200 minutes), the collected charge starts to drop after around 200 min. (Right) Sensor temperature of +30°C. The collected charge decreases rapidly after 35 minutes, but recovers depending on the previously absorbed dose.



**Figure 11.** Change of the leakage current after 5 h of operation of a biased Schottky type CdTe sensor in low flux condition at +15°C (left) and +30°C (right). Hot spot areas as well as highly irradiated areas draw a significantly higher dark current.

Figure 11 shows that pixels in irradiated areas (dashed boxes) are much more likely to exhibit a strong increase in leakage current (more than 10 pA) when the areas have been exposed to doses above 10 kGy (also compare figure 12, right). In the interior of the irradiated area with the highest dose (1079 kGy) the leakage current increases on average up to 58 pA/pixel during the 5 hours of operation at +30°C. Besides the irradiated areas, also single isolated pixels can be found showing a significant higher leakage current after 5 h with values far beyond 30 pA (depicted for +30°C), with respect to the start of the experiment, as shown in figure 11. These hot pixels also maintain a robust charge collection while the counts in the other pixels break down.

Figure 12 indicates that there might be a correlation between the increase of the leakage current and the normalized number of counts, which is also visible in the respective 2d representations

(compare to figure 11, right and figure 8, right). However, the distribution of the leakage current is very broad, hence the leakage current is not the only indicator for polarization resilient pixels. It is worth mentioning that for all pixels an overall increase of the pedestal is observed after a biasing time of 300 minutes in agreement with the raw data analysis in figure 5. Figure 12 (right) depicts the dose dependency of the leakage current increase by displaying the average change of the leakage current of the areas irradiated with different doses at different times after the start of sensor biasing.

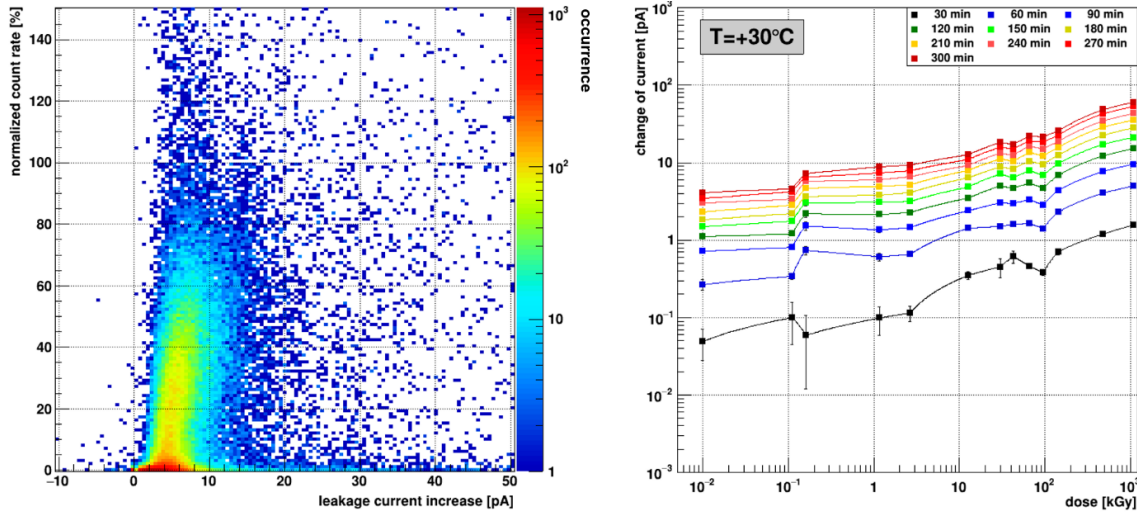


**Figure 12.** (Left) Correlation plot between the leakage current increase (x-axis) and normalized number of counts (y-axis), after 300 minutes at +30°C. As the distribution of the leakage current is very broad there is no strong correlation between leakage current and number of counts. (Right) Increase of the average leakage current per pixel of each ROI as a function of deposited dose for different times after biasing the sensor. Pixels which have been exposed draw a significantly higher leakage current. Please note, that the y-axis is in log scale.

During these measurements, several cycles of five hours of sensor biasing were followed by periods of setting the sensor high voltage to 0 V, called bias refresh, with increasing refresh times (5 s, 30 s, 60 s), totaling an overall sensor biasing time of 20 hours. A bias refresh duration of at least 30 seconds was able to bring the pedestal values back to their initial values, followed by reproducible increase of the pedestal values over time, depending on the sensor temperature. This behavior after a bias refresh was unaltered by longer bias refresh durations.

#### 4.2 Effect of irradiation at the X-ray tube with an acceleration voltage of 25 kV

As bulk damage due to the irradiation with 20 keV photons is highly unlikely [23], the study focuses on radiation effects close to/at the contacts. In a proof-of-concept study, the direct beam of an X-ray tube was used to exclude irradiation effects induced on the pixelated side or ASIC directly, potentially coming from third order harmonics at a beamline. The high voltage of the X-ray tube (with tungsten anode) was set to 25 kV, implying a maximum photon energy of 25 keV and a maximum penetration depth (absorption length 1/e) of about 100  $\mu\text{m}$  in CdTe. A region, defined by a 4 mm thick copper (Cu) plate with a pinhole (about 400  $\mu\text{m}$  in diameter), was irradiated at a temperature of +30°C for 4 hours with a photon flux of around 10<sup>9</sup> ph/mm<sup>2</sup>/s, roughly corresponding

to a dose of 660 kGy (calculated assuming a most probable photon energy of 16.7 keV), comparable to the higher doses of the rectangular shaped areas damaged one year ago.

The photon count and pulse height distributions were determined before and after irradiation, using low flux fluorescence photons from molybdenum in the same way as described before. Figure 13 shows the outcome, indicating clearly similar effects upon irradiation as observed after irradiation at the beamline. The normalized number of hits per pixel (top row) and pulse height spectra (bottom row) of all pixels in the respective areas are plotted as function of the time. Pedestal tracking is applied to correct for the steadily increasing leakage current.

The irradiated pixels show significantly higher counts during the polarization phase (figure 13, center top), starting after around 35 minutes, indicating an increased charge collection in this area, potentially collecting charge from polarized areas close by (figure 13, right). The observed pulse height peak remains relatively stable with a strong increase of the collected charge above the nominal value once the sensor is polarized, leading to a significantly widened pulse height distribution above and below the nominal value of around 610 ADU (corresponding to 17.4 keV Mo photons). The non-irradiated area surrounding the irradiated region behaves as non-irradiated areas in the previous measurements (compare figure 9, left).

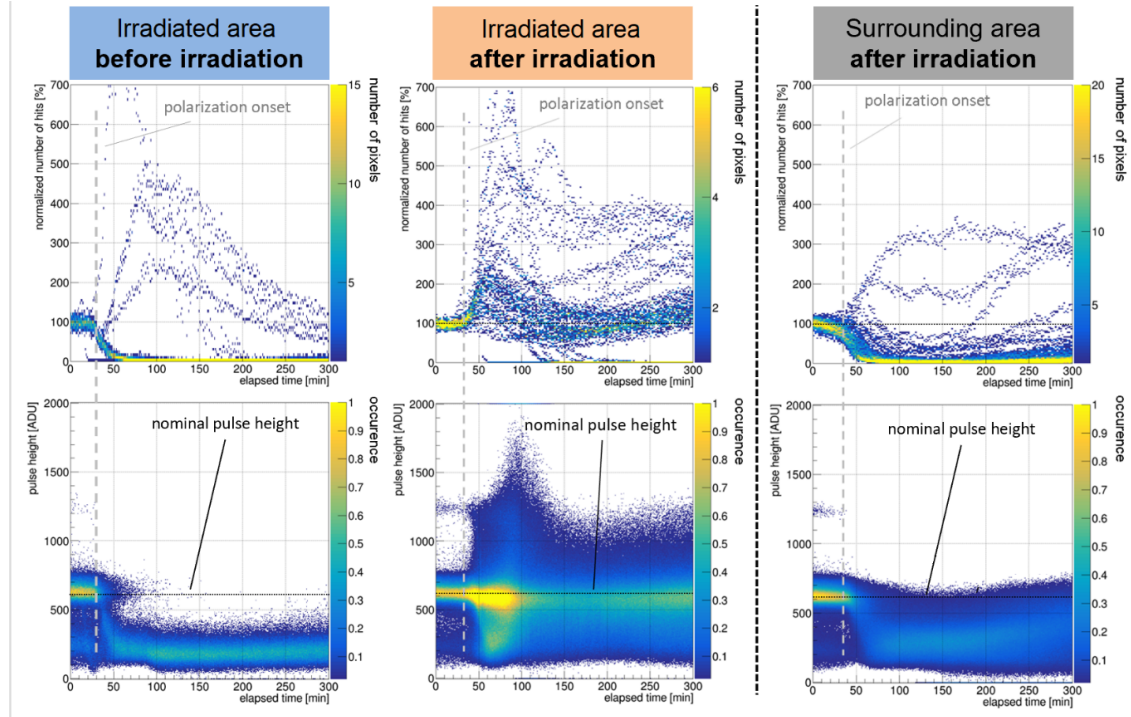


**Figure 13.** Normalized number of photon hits per pixel (top) and the corresponding pulse height histogram (bottom) for the irradiated area before irradiation (left) and after irradiation (center) and its direct surrounding (right) for a Schottky type CdTe sensor. The irradiated area shows higher charge attraction after the polarization onset after 35 min.

#### 4.3 Comparison with ohmic type CdTe sensors

In order to create a more comprehensive picture, an ohmic type CdTe sensor (Pt/CdTe/Pt) was irradiated for 2 hours at the MS beamline using 20 keV photons with fluxes up to  $4 \times 10^{10}$  ph/mm<sup>2</sup>/s,

resulting in an absorbed dose of 1800 kGy. The ohmic type sensor has a platinum (Pt) contact on the irradiated backside, which is identical to the backside contact of the Schottky type sensor used in this study. For evaluating the potential effects of the irradiation, the detector was again exposed to low flux fluorescence photons from molybdenum. Figure 14 shows the pedestal values (bottom) and the normalized number of hits of a sensor section at certain time stamps after the experiment (8 h after the experiment, 2.5 weeks after the experiment, 2.5 month after the experiment). The irradiated area is highlighted in each image by a black rectangle.

Apart from a change in the pedestal (figure 14, top row), no changes in the normalized number of photon hits were observed (figure 14, bottom row), in contrast to what was measured in this study with Schottky type CdTe sensors. Furthermore, the leakage current of Schottky type sensors increases as a function of deposited dose (cf. figure 11), whereas the ohmic type sensor shows a slight decrease in the pedestal although being exposed to an even higher dose.

8 h after the end of the irradiation (figure 14, left), all affected pixels shift to higher values, indicating the collection of more electrons with respect to the situation before the irradiation, which is likely an afterglow phenomenon due to the detrapping of charge carriers from deep level traps. However, the pixel rows which have absorbed the highest doses due to a non-uniform beam profile (pixel rows 70–80), exhibit a relatively low increase of their pedestal values. After storing the ohmic type sensors in ambient conditions for 2.5 weeks (figure 14, center), the afterglow phenomena completely vanished. A lower pedestal value, corresponding to a lower dark current, is obtained for the high dose area (pixel rows 70–80) as a left over, with marginal changes in the longer-term (2.5 months, figure 14, right).

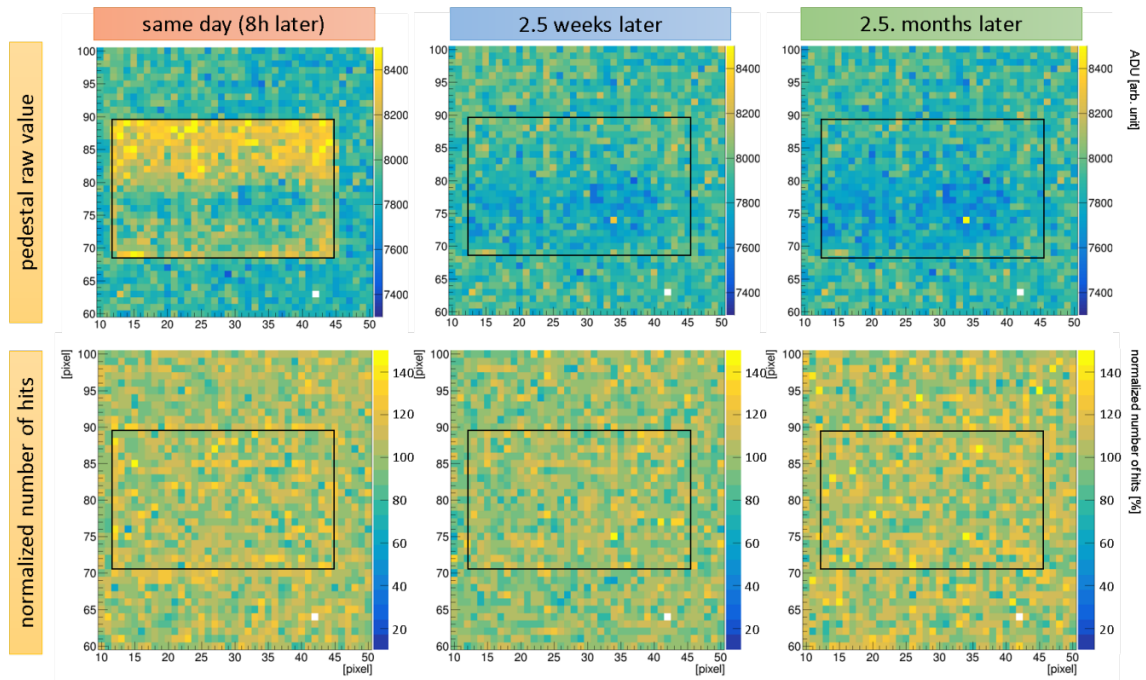


**Figure 14.** Pedestal images (top) and normalized number of hits (bottom) for an ohmic type CdTe sensor after a high irradiation dose at different times after the irradiation.

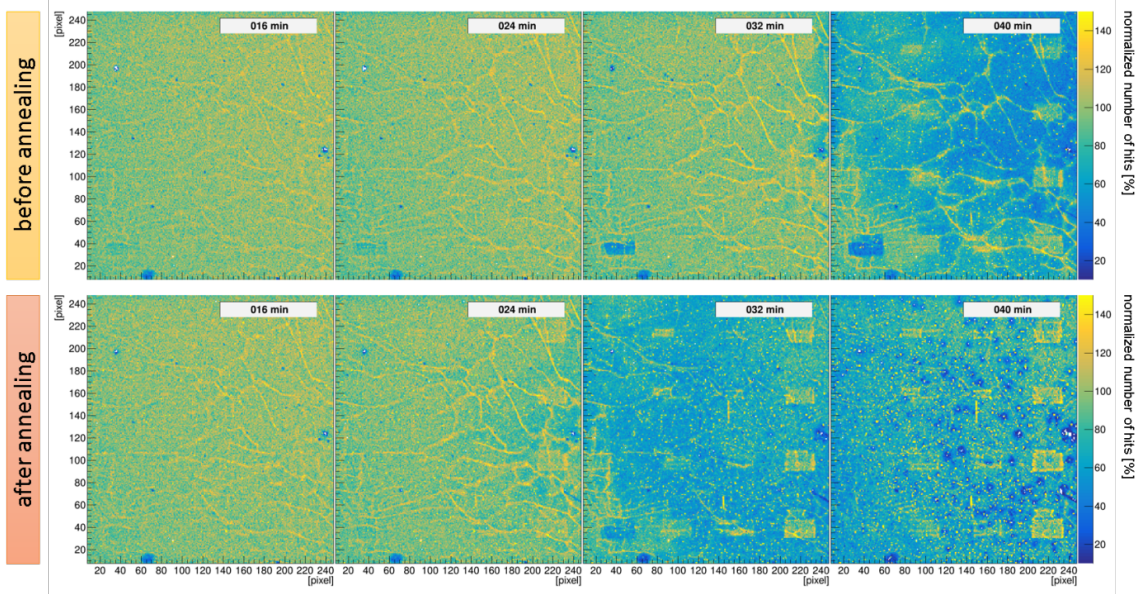


**Figure 15.** Snap shots of the normalized photon hit maps of a Schottky type CdTe sensor before (top) and after (bottom) annealing operated at  $-500$  V in low flux conditions at  $+30^{\circ}\text{C}$  at different time stamps.

#### 4.4 Effect of thermal annealing at $+80^{\circ}\text{C}$

Thermal annealing, initially foreseen to investigate a possible recovery process of the irradiated areas, turned out to alter the polarization characteristics of a Schottky type CdTe sensor. A Schottky type CdTe sensor was annealed for 10 h at  $+80^{\circ}\text{C}$  in ambient conditions with a slow ramp up and cool down phase.

Changes were found for the onset of the polarization process, which starts significantly earlier in the annealed case. Figure 15 shows snapshots of the normalized photon hit maps for the same sensor before (top) and after annealing (bottom). Whereas the situation is still comparable 16 min after being biased at  $-500$  V, the annealed sensor shows first clear signs of polarization already after 24 min. After 32 min, large areas of the thermally annealed sensor count significantly less photons compared to the initial situation (and the situation before annealing) and after around 40 min first circular sinks, collecting significantly less to no charge, appear.

Regardless of a faster polarization and its potential drawback, the annealed sensor appears to reach a stable behavior. After 200 min no significant change in the pixel hit distribution is visible for the last hour as shown in figure 16. Although almost all pixels count below 50% (blue) of the initial hits after 60 minutes, the distribution of the number of counts remains relatively stable. On the contrary, before being annealed, the sensor gives rise to large areas with less than 10% of the initial photon hits (top left, white areas) when polarized and no stable state was reached in the 5 h time (figure 16, center top). Note that no specific change is observed for the irradiated areas due to annealing.

A change of the charge collection behavior can also be seen in figure 17. The same sensor has been analyzed before and after annealing, including all pixels from the pixel matrix except the irradiated areas. The temporal evolution of the pulse height spectra (figure 17, bottom row) confirms

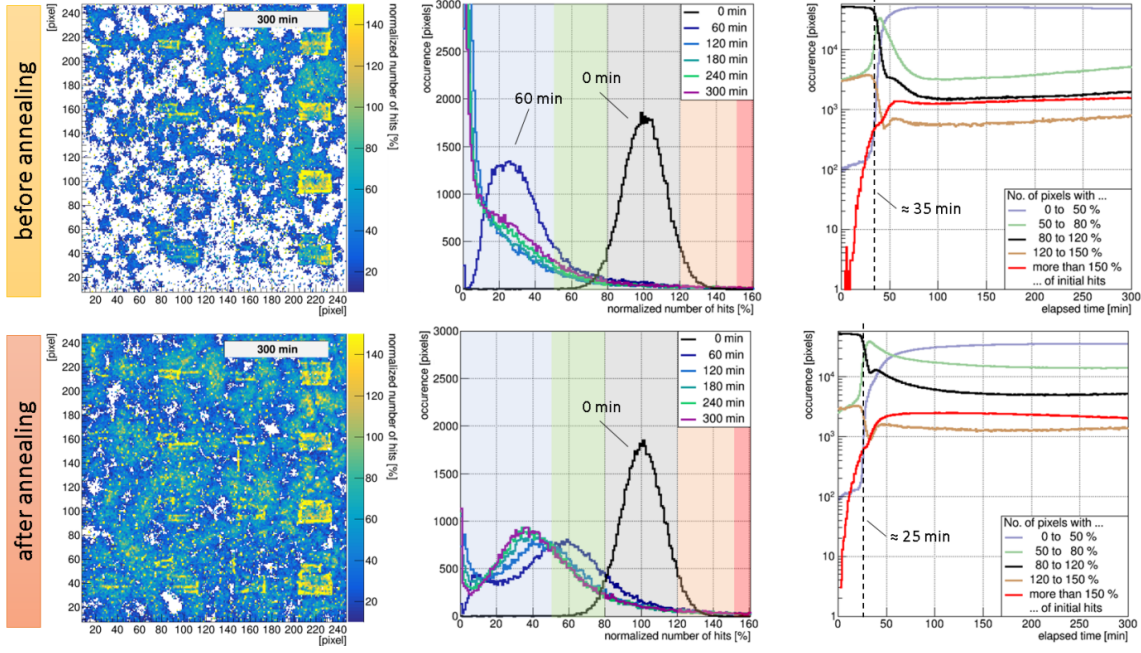


**Figure 16.** (Left) Response maps of a Schottky type CdTe sensor after 5 h operated at  $-500$  V in a low flux environment at  $+30^{\circ}\text{C}$ , (top) before and (bottom) after annealing. (Center) Corresponding pixel hit distribution at different time stamps. (Right) Evaluation of the pixel hit distribution according to defined categories versus experiment time.

the earlier onset of the polarization (post-annealing: 25 min/pre-annealing: 35 min). Additionally, a more robust photo peak can be observed (figure 17, bottom center) compared to the pre-annealed case, where the photo peak smears out during the measurement (figure 17, bottom left).

That finding is also reflected in the plots of the evolution of the photon counts (figure 17, top right) and of the collected charge (figure 17, bottom right). After annealing the sensor, a significant number of pixels reach a stable counting plateau of around 45% of the initial counts.

#### 4.5 Comparison between different batches of electron collecting Schottky CdTe sensors

In order to see if differences of the CdTe material change the polarization behavior in Schottky type CdTe sensors, a sensor from a batch from 2017 was tested, which went through the same measurement process at the MS beamline and was subsequently irradiated to similar doses as the sensor measured before. The results from the material from the 2017 batch differ from recent material from 2019 in several aspects, starting from a higher leakage current (cf. table 2), as shown in figure 18: the onset of the polarization is more distinct in the 2019 batch material (after around 35 min), whereas a deterioration of the nominal number of photon hits (black line) is observed for the 2017 batch material from the very beginning (right column). After 60 min, the 2019 batch material still shows a Gaussian like distribution profile (with an average of 20% of the initial average number of photon hits) retaining a pronounced shoulder over the full 5 h time period (center column).

Furthermore, the 2017 batch Schottky type CdTe sensor material shows a much higher granularity of hot pixels compared to the more recent sensor material as shown in figure 18 (left column).

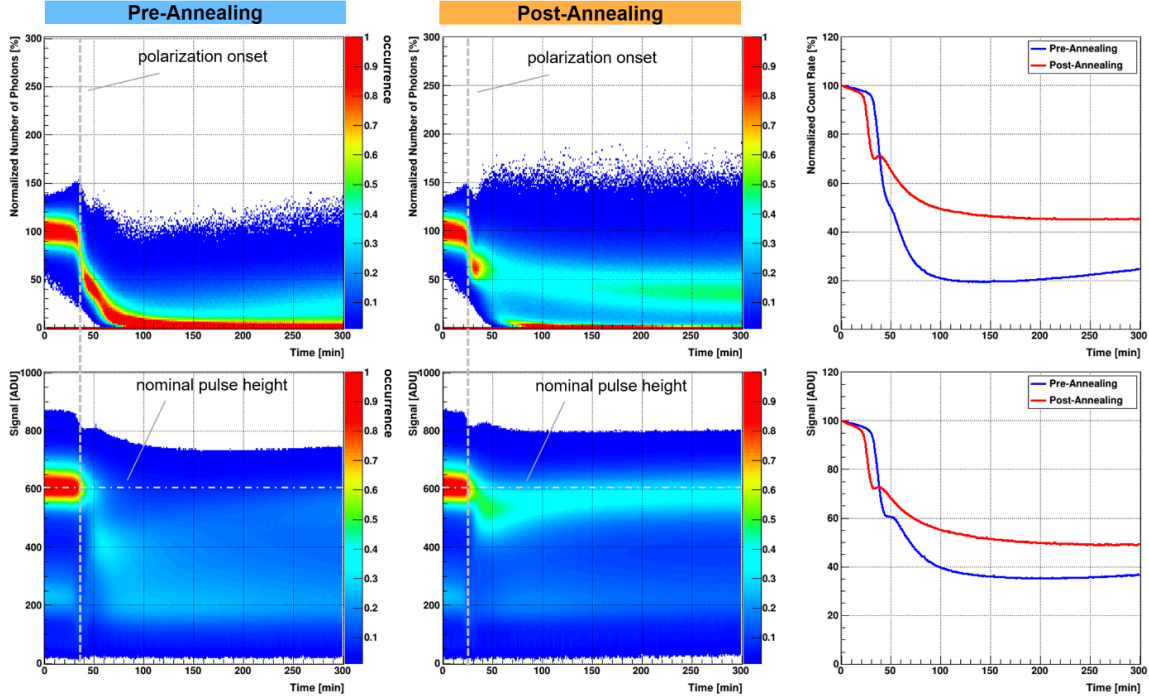


**Figure 17.** Temporal evolution of the (top) photon counts and (bottom) pulse height spectra for all pixels (except the irradiated regions) (left) before annealing and (center) after annealing. The temperature of the sensor was  $+30^{\circ}\text{C}$ . (Right) Direct comparison between (top) the normalized photon counts and (bottom) the average collected charge before and after thermal annealing.

**Table 2.** Sensor current of Schottky type CdTe sensors (2017 and 2019 batch) biased at  $-500\text{ V}$  and at  $+30^{\circ}\text{C}$ , measured with a Keithley high voltage source.

Batch	2017	2019
Sensor current (after biasing at 0 min)	$3.06\text{ }\mu\text{A}$	$0.92\text{ }\mu\text{A}$
Lowest sensor current (after 2–3 min)	$1.75\text{ }\mu\text{A}$	$0.65\text{ }\mu\text{A}$
Sensor current (after 5 h)	$9.39\text{ }\mu\text{A}$	$2.72\text{ }\mu\text{A}$

## 5 Conclusion

A comprehensive study of the influence of irradiation with low energy X-rays on Schottky type CdTe sensors regarding its bias-induced polarization behavior is presented. Based on in-situ photon hit maps the deterioration of the sensors capability to detect photons was monitored. Whereas no indication for bias-induced polarization was found in ohmic type sensors, a clear temperature dependence could be visualized for Schottky type sensors with a significant increase of the leakage current over the biasing time and a more robust charge collection of irradiated areas.

Our results show that shallowly penetrating X-rays are capable to alter the polarization characteristics of a Schottky type CdTe sensor. A significantly more robust charge collection and correspondingly higher photon counts were found in preirradiated areas. Furthermore, this study indicates that a fully irradiated Schottky type sensor could provide a suitable environment to mea-

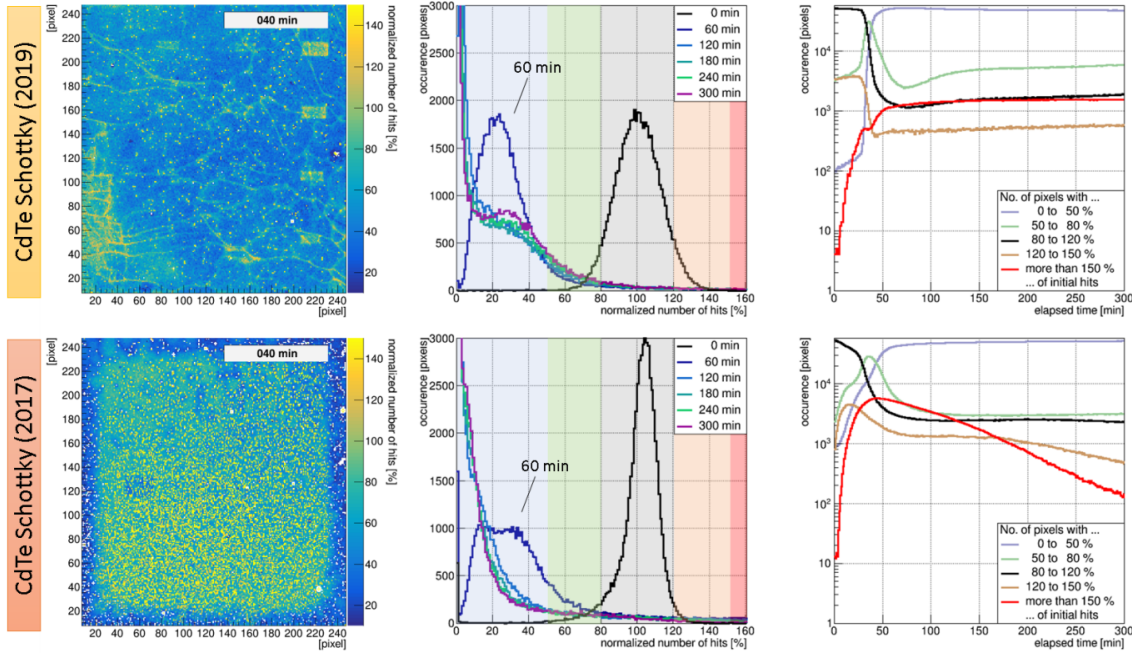


**Figure 18.** (Left) Response maps of two Schottky type CdTe sensor (2017 and 2019 batch) after 40 min operated at  $-500$  V in a low flux environment at  $+30^{\circ}\text{C}$ . (Center) Corresponding pixel hit distributions at defined time stamps. (Right) Evaluation of the pixel hit distribution according to defined categories versus experiment time (right) 0–50% of initial hits: very low — blue; 50–80%: low — green; 80–120%: nominal — black; 120–150%: high — orange; above 150%: very high — red.

sure on a stable plateau with the drawback of an increased leakage current. In contrast to a changing polarization environment, corrections can be applied to correct for response non-uniformities under such stable circumstances.

Further experiments have to reveal the long-term stability of the irradiation effects and whether irradiation with doses beyond those investigated in this study might lead to overcompensation.

The polarization process of Schottky type sensors is also influenced by thermal annealing. Even though sensor annealing triggers a faster polarization, an overall more stable situation is reached after 240 min at  $+30^{\circ}\text{C}$ .

An ohmic type CdTe sensor with the same backside contact (Pt) as the Schottky type sensors shows no variation between heavily irradiated and non-irradiated areas regarding the number of photon hits. Whereas the radiation effects in Schottky type sensors are still visible one year after the irradiation, the radiation effects in ohmic type sensors are relatively short-term effects lasting only a few weeks. As we used photon energies not exceeding 25 keV (shallow penetration), thus being able to exclude bulk damage as well as radiation damage to the readout chip, we consider it worth to study the influence of the contacts on the polarization behavior in more detail in order to understand the substantial change upon irradiation in Schottky type CdTe sensors.

## Acknowledgments

This project has received funding from the European Union’s Horizon 2020 research and innovation program under the Marie Skłodowska-Curie grant agreement no. 884104 (PSI-FELLOW-III-3i).

## References

- [1] M.J. Berger et al., *XCOM: Photon Cross Section Database. Version 1.5*, National Institute of Standards and Technology, Gaithersburg, MD, U.S.A. (2010).
- [2] G. Nasser et al., *The use of Schottky CdTe detectors for high-energy astronomy: application to the detection plane of the instrument SVOM/ECLAIRs*, *Proc. SPIE* **9144** (2014) 91443X.
- [3] C. Ullberg, M. Urech, N. Weber, A. Engman, A. Redz and F. Henckel, *Measurements of a dual-energy fast photon counting CdTe detector with integrated charge sharing correction*, *Proc. SPIE* **8668** (2013) 86680P.
- [4] T. Hirono et al., *Development of a CdTe pixel detector with a window comparator ASIC for high energy X-ray applications*, *Nucl. Instrum. Meth. A* **650** (2011) 88.
- [5] G. Sun, H. Samic, J. Bourgoïn, D. Chambellan, O. Gal and P. Pillot, *A comparison between GaAs and CdTe for x-ray imaging*, *IEEE Trans. Nucl. Sci.* **51** (2004) 2400.
- [6] D. Greiffenberg et al., *Characterization of GaAs:Cr sensors using the charge-integrating JUNGFRÄU readout chip*, *2019 JINST* **14** P05020.
- [7] D. Greiffenberg, *Charakterisierung von CdTe-Medipix2-Pixeldetektoren*, Ph.D. Thesis, Albert-Ludwigs-University, Freiburg, Germany (2010).
- [8] E. Hamann, *Characterization of high resistivity GaAs as sensor material for Photon Counting Semiconductor Pixel Detectors*, Ph.D. Thesis, Albert-Ludwigs-University, Freiburg, Germany (2013).
- [9] P.J. Sellin, *Recent advances in compound semiconductor radiation detectors*, *Nucl. Instrum. Meth. A* **513** (2003) 332.
- [10] S. Del Sordo, L. Abbene, E. Caroli, A.M. Mancini, A. Zappettini and P. Ubertini, *Progress in the development of CdTe and CdZnTe semiconductor radiation detectors for astrophysical and medical applications*, *Sensors* **9** (2009) 3491.
- [11] P. Zambon et al., *Spectral response characterization of CdTe sensors of different pixel size with the IBEX ASIC*, *Nucl. Instrum. Meth. A* **892** (2018) 106.
- [12] V. Gnatyuk, O. Maslyanchuk, M. Solovan, V. Brus and T. Aoki, *CdTe X/γ-ray detectors with different contact materials*, *Sensors* **21** (2021) 3518.
- [13] M. Ruat and C. Ponchut, *Defect signature, instabilities and polarization in CdTe X-ray sensors with quasi-ohmic contacts*, *2014 JINST* **9** C04030.
- [14] A. Cola and I. Farella, *The polarization mechanism in CdTe Schottky detectors*, *Appl. Phys. Lett.* **94** (2009) 102113.
- [15] P. Siffert et al., *Polarization in Cadmium Telluride Nuclear Radiation Detectors*, *IEEE Trans. Nucl. Sci.* **23** (1976) 159.
- [16] H. Toyama, A. Higa, M. Yamazato, T. Maehama, R. Ohno and M. Toguchi, *Quantitative analysis of polarization phenomena in CdTe radiation detectors*, *Jpn. J. Appl. Phys.* **45** (2006) 8842.
- [17] A. Meuris, O. Limousin and C. Blondel, *Characterization of polarization phenomenon in Al-Schottky CdTe detectors using a spectroscopic analysis method*, *Nucl. Instrum. Meth. A* **654** (2011) 293.
- [18] R.O. Bell, G. Entine and H. Serreze, *Time-dependent polarization of CdTe gamma-ray detectors*, *Nucl. Instrum. Meth.* **117** (1974) 267.
- [19] P.R. Willmott et al., *The Materials Science beamline upgrade at the Swiss Light Source*, *J. Synchrotron. Radiat.* **20** (2013) 667.

- [20] A. Mozzanica et al., *The JUNGFR AU detector for applications at synchrotron light sources and XFELs*, *Synchrotron Radiat. News* **31** (2018) 16.
- [21] M. Funaki, Y. Ando, R. Jinnai, A. Tachibana and R. Ohno, *Development of CdTe detectors in Acrorad*, (2007) and online pdf version at [https://www.acrorad.co.jp/dcms\\_media/other/Development%20of%20CdTe%20detectors%20in%20Acrorad.pdf](https://www.acrorad.co.jp/dcms_media/other/Development%20of%20CdTe%20detectors%20in%20Acrorad.pdf).
- [22] A. Gädda et al., *Advanced processing of CdTe pixel radiation detectors*, *2017 JINST* **12** C12031.
- [23] M. Moll, *Radiation Damage in Silicon Particle Detectors*, Ph.D. Thesis, University of Hamburg, Hamburg, Germany (1999).
- [24] S. Cartier et al., *Micron resolution of MÖNCH and GOTTHARD, small pitch charge integrating detectors with single photon sensitivity*, *2014 JINST* **9** C05027.
- [25] V. Astromskas, E.N. Gimenez, A. Lohstroh and N. Tartoni, *Evaluation of Polarization Effects of  $e^-$  Collection Schottky CdTe Medipix3RX Hybrid Pixel Detector*, *IEEE Trans. Nucl. Sci.* **63** (2016) 252.
- [26] K. Okada, Y. Sakurai and H. Suematsu, *Characteristics of both carriers with polarization in diode-type CdTe x-ray detectors*, *Appl. Phys. Lett.* **90** (2007) 063504.